Model insights into EEG origin under transcranial direct current stimulation (tDCS) in the context of psychosis

Joséphine Riedinger, Axel Hutt

MDPI

Article

Model insights into EEG origin under transcranial direct current stimulation (tDCS) in the context of psychosis

Joséphine Riedinger [1,2,†,‡], Axel Hutt [1,†,‡]

[1] Université de Strasbourg, CNRS, Inria, ICube, MLMS, MIMESIS, F-67000 Strasbourg, France
[2] INSERM, U1114, Neuropsychologie cognitive et physiopathologie de la schizophrénie, 67085, Strasbourg
* Correspondence: axel.hutt@inria.fr
† Current address: Affiliation 1
‡ A. Hutt and J. Riedinger have contributed equally to the work.

Abstract: Schizophrenia is a psychotic disease that develops progressively over years with a transition from prodromal to psychotic state associated with a disruption in brain activity. Transcranial Direct Current Stimulation (tDCS), known to alleviate pharmaco-resistant symptoms in patients suffering from schizophrenia, promises to prevent such a psychotic transition. To understand better how tDCS affects brain activity, we propose a neural cortico-thalamo-cortical (CTC) circuit model involving the Ascending Reticular Arousal System (ARAS) that permits to describe major impact features of tDCS, such as excitability for short-duration stimulation and electroencephalography (EEG) power modulation for long-duration stimulation. To this end, the mathematical model relates stimulus duration and Long-Term Plasticity (LTP) effect, in addition to describing the temporal LTP decay after stimulus offset. Moreover, we reproduce successfully EEG-power modulation under tDCS in a ketamine-induced psychosis model and confirm the N-methyl-d-aspartate (NMDA) receptor hypofunction hypothesis in the etiopathophysiology of schizophrenia. The model description points to an important role of the ARAS and the $\delta-$ rhythm synchronicity in CTC circuit in early stage psychosis.

Keywords: tDCS, ketamine, psychotic transition, EEG, modelling, thalamocortical circuit

Citation: Riedinger, J.; Hutt, A. EEG under tDCS. *J. Clin. Med.* **2021**, *1*, 0. https://doi.org/

Received:
Accepted:
Published:

1. Introduction

Schizophrenia is a psychotic disease that affects almost 1% of the worldwide population. This disorder has a multifactorial etiology which includes environmental and genetic factors, and develops progressively along years before to manifest generally between 15 and 25 years old. During the prodromal pre-psychotic phase, first low-intensity psychotic/positive symptoms insidiously appear [1,2]. About one-third of the at-risk mental state patients will experience the psychotic transition, marked by the intensification and worsening of psychotic symptoms over almost 2 years. This frequently culminates in an acute episode of psychosis, and finally resulting to the chronicisation of the psychotic syndromes [1,3,4]. For patients diagnosed with schizophrenia, pharmacological and psychological therapy allow to alleviate symptoms and significantly improve patients every-day-life. Nevertheless, finding treatments to prevent the psychotic transition would be a precious lever for patients and psychiatry.

One of the promising non-invasive preventive approaches is the transcranial Direct Current Stimulation (tDCS). It modulates neuronal activity by electric currents and is efficient in the reduction of pharmaco-resistant psychotic and negative symptoms, as well as improvement of cognitive performance in patients and healthy subjects [5–7]. For instance, in patients suffering from schizophrenia long-lasting (several months) and robust reduction of negative and positive symptoms with low side-effects have been observed after application an anodal tDCS protocol of few days [5,8,9]. While a large number of studies

demonstrate the powerful potential of the tDCS as a treatment for psychotic disorder, the questions of whether and how psychosis can be prevented by tDCS remains open. To get closer to this aim, it is mandatory to understand better the mechanism of action and electrophysiological influence of tDCS on neuronal networks.

The dysconnection hypothesis in schizophrenia allows to reveal links between the pathophysiology of the disease and clinical signs, and indicates inter- and intra-structural impairments in functional integration processes [10,11]. Indeed, Cortico-Thalamo-Cortical (CTC) dysfunctions and disturbance in functionally associated neuronal oscillations were reported from the prepsychotic phase of schizophrenia. These oscillopathies encompass an increased power of prefrontal resting state activity in the broadband $\gamma-$frequency (30 - 80 Hz) [12,13], as well as a reduced power in cortical low-frequency oscillations, like in the $\delta-$ band (1 - 4 Hz) [14,15] and in non-REM sleep spindles occurring in the $\sigma-$ frequency band (10 - 17 Hz) [16,17].

Interestingly, some of these prodrome-related osccillopaties can be transiently reproduced in humans and rodents by a sub-anesthetic administration of the N-methyl-d-aspartate (NMDA) receptor antagonist ketamine. A single sub-anesthetic dose of ketamine induces psychotomimetic effects in healthy humans [18] and worsen positive symptoms in patients suffering from schizophrenia [19]. Moreover, electrophysiological studies in rats [20–22] and humans [23–25] showed that such a psychotomimetic ketamine administration disrupts the CTC functional dynamics, and induces an increased power of $\gamma-$ oscillations and a reduced power of slow wave, an effect reversed by the antipsychotic action of clozapine [26]. Therefore, the sub-anesthetic ketamine provide a reliable animal model of a transition to a psychosis-relevant state [27], and support the dysconnection hypothesis for the etiopathophysiology of schizophrenia, more precisely *via* an hypofunction of the NMDA receptors [28].

Here, we propose to explain the impact of anodal tDCS on psychotic brain dynamics by the use of a mathematical model of the CTC circuit. This model encompasses the CTC connectivity topology, as well as excitatory and inhibitory neuronal populations in the network structures. At first, we have reproduced typical activity modulations by tDCS, such as excitability and EEG power spectrum, to validate the neural model. Then, the psychosis network dynamic is mimicked by modeling the action of ketamine on glutamatergic neurotransmission. Finally, tDCS application in the context of psychosis has been simulated and forecasts of tDCS action on CTC structures are provided. The neuromodulatory action of tDCS has been modeled by a cortical constant input and a change in the neuronal population transfer function. Cortical electroencephalograms (EEG) have been computed numerically for all conditions and compared with literature. We shed light on the essential neural mechanisms and CTC interactions that allow to mimic prodrome-related oscillopathies and the observed effect of tDCS in psychotic patients.

2. Materials and Methods

2.1. The model

It is well-established that EEG originates from population activity in cortical layers [29, 30]. Neural ensemble models are well-known to provide a very good description of EEG [30–33]. The model employed describes population activity in the supragranular cortex layers I-III (SG) and the cortico-thalamic loop between granular/infragranular cortical layers IV-VI (GIG), the thalamic relay cells and the reticular structure, see Appendix for details. The network is sketched in Fig. 1. SG cells receive input from the brainstem, or more generally from the Ascending Reticular Arousal System (ARAS) [34,35], and cells in input layer IV exhibit afferent connections from thalamic structures and connect to infragranular cortical cells in layers V and VI (Fig. 1(A)). Moreover, the GIG cells receive input from thalamic relay cells in the CTC and project back to thalamic relay and reticular cells, cf.

Fig. 1(B). GABAergic neurons in the reticular nucleus receive excitatory inputs from GIG pyramidal cells and thalamic relay neurons, while the inhibitory reticular outputs are send to the thalamic relay cells.

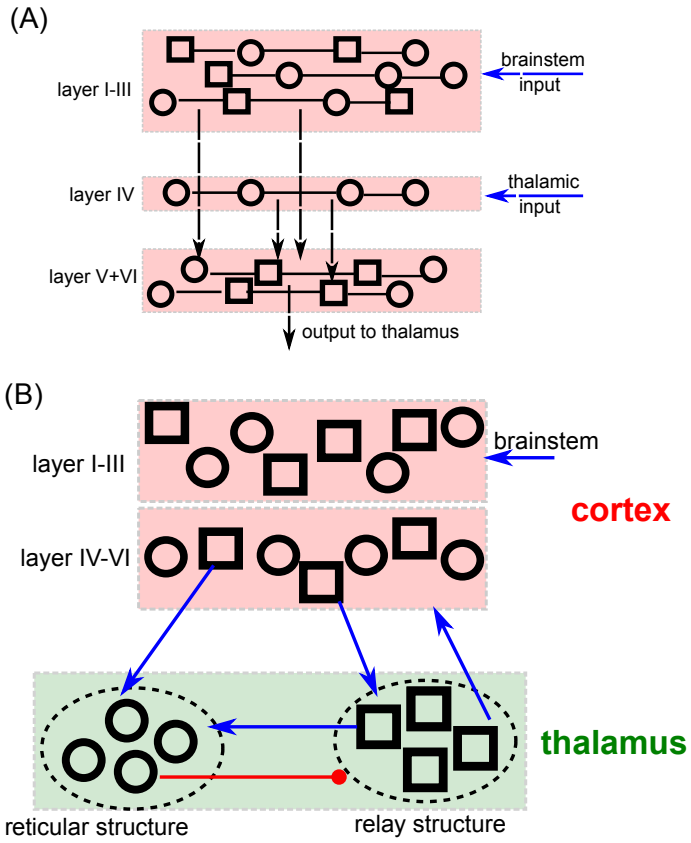

Figure 1. Cortico-thalamo-cortical network model of neural populations. (A) The supragranular layers I-III, granular layer IV and infragranular layers V and VI exhibit excitatory (represented by squares) and inhibitory (circles) neurons. (B) Blue and red connections between cortex and thalamic structures denote excitatory and inhibitory synaptic connections. The reticular and relay structures includes inhibitory (circles) and excitatory (squares) neurons, respectively.

The principal brain rhythms investigated in the present study are the $\delta-$ $(1-4\text{Hz})$, $\sigma-$ $(10-17\text{Hz})$ and the $\gamma-$ rhythm $(30-80\text{Hz})$. Following previous modeling studies [32,36–38], we hypothesize that the $\delta-$ and $\sigma-$ rhythms originate in the cortico-thalamic circuit (including both thalamic and GIG structures), whereas $\gamma-$rhythms are generated in the SG layers [38,39] in accordance to experimental findings [40]. The proposed model considers interactions of excitatory and inhibitory local networks as the major rhythm origin in line with previous modeling studies [41,42].

2.2. The action of transcranial Direct Current Stimulation

Transcranial Direct Current Stimulation is a neuromodulatory noninvasive brain stimulation tool [43,44] known to be able to alleviate patients from symptoms in schizophrenia [5,8,9], major depression [45] or autism [46]. It generates a constant current between two electrodes and current polarity distinguishes anodal and cathodal tDCS (a-tDCS and c-tDCS).

To understand and describe the action of tDCS by a model, it is important to distinguish short and long stimulations. Short applications, i.e. from seconds to a few minutes, of tDCS result in altered membrane resting potentials and excitability shifts during stimulation but no long-term after-effects [43,47]. A-tDCS increases excitability and the resting potential, whereas c-tDCS diminish both excitability and resting potential. The present work considers primarily a-tDCS and implements its impact by an increase of constant

input and steepness decrease of transfer functions of both neuron types in all cortical layers. As demonstrated in previous studies [39,48], the synchronous impact on both input and transfer function steepness is a direct result of a modulation by Poisson spiking activity in the ensemble, cf. the Appendix.
The excitability effect by tDCS has been demonstrated experimentally by several previous studies [47,49]. Typically, neural responses are evoked by a different experimental stimulus, such as transcranial magnetic stimulation (rTMS). Anterior experimental research has demonstrated the increased (decreased) evoked response magnitude with increasing a-tDCS (c-tDCS) current. To describe this effect, we have implemented a transient external stimulation and evaluate the systems response magnitude and its baseline level subject to the model tDCS current. Here, we model a-tDCS and c-tDCS currents by model currents $I_{\text{tDCS}} > 0$ and $I_{\text{tDCS}} < 0$, respectively.

Conversely, stimulation of several minutes or longer can elicit prolonged after-effects of several hours [44,50]. These prolonged plasticity effects request neural action evolving on a larger time scale than the synaptic short-time action. A good candidate is Long Term Potentiation (LTP), that has indeed been found as a probable underlying long-term mechanism in long-stimulation a-tDCS [51,52]. The plasticity is triggered by anodal tDCS-induced neural synchronization that induces complex dynamics of diverse ion channels, cascade signaling and protein transcriptions. We describe the overall impact as an enhanced excitatory synaptic efficacy in accordance to previous studies [51–53]. To this end, we introduce a factor f_{tDCS} for the excitatory synaptic efficacy in both supra- and infra-granular layers, cf. the Appendix for more details.

2.3. The action of ketamine

The anesthetic ketamine induces several diverse neural actions [54–56]. For instance, it antagonizes NMDA-receptors in cortical and subcortical structure, increases the cortical and subcortical glutamate concentration and affects the cortical dopamine system mammals. As a major effect, at sub-anesthetic doses it is known to enhance the excitability level in cortical and subcortical structures, possibly through disinhibition of excitatory cortical pyramidal neurons [57,58].
Since the balance between excitation and inhibition impacts the oscillatory brain activity, it is expected that ketamine modulates the EEG power spectrum. Indeed, ketamine induces increased gamma power and a decreased power in lower delta frequency bands in humans [23] and rats [20,21,58,59]. Moreover, a general $\delta-$ power reduction has been observed in the entire CTC circuit [26,58]. Recent experimental studies on a slow-wave sleep model in rats has shown a decrease of frontoparietal spectral power in the σ-frequency band [26,60]. We have implemented the ketamine modulation of excitation and inhibition on neural populations, cf. the Appendix, to reproduce the EEG power spectrum modulation observed in previous experimental studies.

2.4. Functional connectivity

Our model network includes connected neural populations. To learn more on the interaction among these populations, we evaluate the functional connectivity (FC) between them. FC quantifies the time-dependent degree of interaction between two populations. Several measures have been proposed to quantify it [61], such as spike-field coherence [37] or other synchronization indices. We consider here the time-averaged phase coherence [37, 62] which represents the phase-locking value (PLV) [63] between two time series with $0 \leq \text{PLV} \leq 1$. These time series represent the activity of different populations in different frequency bands. It has been shown recently [64], that phase synchronization quantifies the degree of information sharing in noise-driven models. For $\text{PLV} = 1$, two time series are completely phase locked and their populations activity is maximum synchronized, whereas $\text{PLV} = 0$ reflects a complete activity de-synchronization. The larger the phase coherence

PLV, the larger is the functional connectivity between two populations and the more the two populations interact.

3. Results

3.1. Excitability

Excitability modification is one of the major features of short-term tDCS. Figure 2 shows model simulations of an event-related potential (ERP) (A) and its impact on the resting state activity (B). We observe an augmented excitability for a-tDCS in the ERP. For both GIG cortical and thalamic relay neurons, short-term tDCS induce an increased (decreased) resting membrane potential for a-tDCS (c-tDCS). Conversely, the resting firing rate is poorly affected. These results are in good accordance to previous experimental observations [43,47].

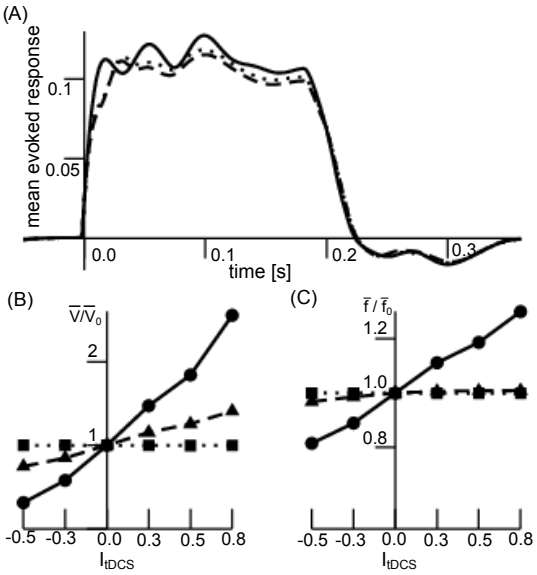

Figure 2. tDCS-induced excitability. (A) The evoked potential time course is shown for tDCS input current $I_{\text{tDCS}} = 0.0$ (dashed), $I_{\text{tDCS}} = 0.3$ (dotted) and and $I_{\text{tDCS}} = 0.8$ (solid). The larger I_{tDCS}, the larger is the response magnitude during transient stimulation (up to $\sim$ 200ms). After stimulation, the system response is almost identical for all input currents. (B) The relative baseline resting potential (left panel) and firing rate (right panel) in the precursor time interval 50ms before stimulation input. The value $\bar{V}_0(\bar{f}_0)$ is the baseline resting potential (resting firing rate) for absent input currents. The lines denotes the summed up relative cortical resting activity in the cortical GIG neurons (solid line), in the excitatory relay cells (dashed line) and the reticular cells (dotted line). We observe an increase of the resting membrane potential (left) for $I_{\text{tDCS}} > 0$ (a-tDCS) and a decrease for $I_{\text{tDCS}} < 0$ (c-tDCS) in cortical and relay cells, whereas no impact on reticular cells is found. Conversely, the resting firing rate is poorly modulated by the tDCS current.

3.2. Anodal tDCS-effect on spectral power

Long duration a-tDCS stimulation is known to yield cognitive enhancement [6], induces LTP [53] and may serve an important role in clinical psychiatry in the future [5,8,9,65]. To describe the involved plasticity, we have developed a model that relates tDCS duration and plasticity effect. Figure 3 (A,left panel) shows the major model idea: for short stimulation duration, no plasticity is present, while the impact increases with longer stimulation. It has also been found experimentally, that the plasticity impact saturates after some time, i.e. the long-term effect of tDCS does not change anymore [44,66]. After a-tDCS offset, the plasticity reduces but much slower, see Fig. 3 (A,right panel). The understanding of both enhanced and diminished plasticity in the course of time is important since a-tDCS stimulation protocols alternate between stimulation with a certain duration and current intensisty, and stimulation pauses. Our temporal model postulates the tDCS impact on

plasticity strength subjected to stimulation time and stimulation pauses. Figure 3(B) shows the impact of the single stimulation duration in a stimulation sequence on the plasticity, similar to the tDCS studies described in [44]. We observe an increase in plasticity strength f_{plast} with increasing stimulation duration T_s and hence a prolonged long-term effect after stimulation offset. For details on the numerical implementation, please see the Appendix.

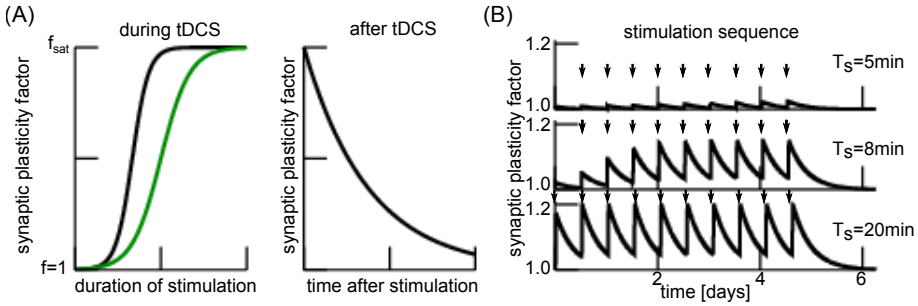

Figure 3. Modelled plasticity impact during and after anodal tDCS stimulation. (A) *Left panel:* very short stimulus duration does not induce any plasticity (the synaptic plasticity factor is $f \approx 1$), medium duration exhibits a strong plasticity effect ($1 \leq f \leq f_{\text{sat}}$) that does not enhance anymore for long duration stimuli [44] ($f \to f_{\text{sat}}$) with saturation factor f_{sat}. For high and low a-tDCS currents (black and green curve, resp.), the qualitative behavior is similar, but it takes more time to induce the same plasticity effect for lower a-tDCS currents [66]. Our model describes this temporal evolution of plasticity effect by a population growth model, see Appendix for more details. *Right panel:* after stimulation offset the plasticity effect diminishes exponentially with time. Experimental studies [66] indicate that the decay time scale is in the range of tens of minutes for typical previous stimulation current ($\sim 0.5 - 1$mA). (B) Simulation of the plasticity effect in a typical a-tDCS sequence motivated by [44]. Arrows indicate stimulation periods. A single a-tDCS period had a duration T_s with a stimulation pause of 12 hours, 10 repetitions and a final period of 34 hours, cf. Appendix for more details. Further parameters are $\tau_{\text{plast}} = 3$h and $\tau_{\text{decay}} = 500$h.

The plasticity effect is accompanied by spectral power enhancement, as shown in Fig. 4. We demonstrate that long duration a-tDCS induces EEG power enhancement in the $\delta-$, $\sigma-$ and $\gamma-$ frequency range, which decreases with time after the stimulation ends. Experimental observations during sleep in healthy subjects similarly report an increased power of the sigma frequency band after a slow oscillatory a-tDCS application [67,68]. Moreover, it is show in [69] that oscillations in the delta frequency band are enhanced following a-tDCS.

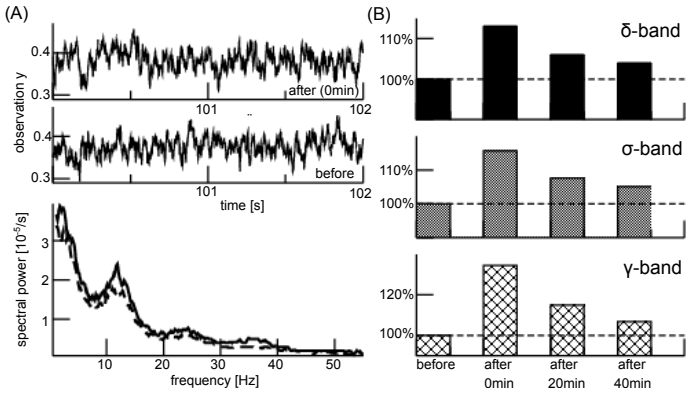

Figure 4. Long duration-anodal tDCS impact on EEG. (A) Upper panels: simulated EEG time traces before a-tDCS stimulation and immediately after. Lower panel: the corresponding power spectral density distributions for activity before (dashed line) and immediately after (solid line) stimulation. (B) Relative power change with respect to power before stimulus for different time periods after stimulation. Plasticity effects are modeled by an increase of excitatory efficacy with factors $f_{\text{tDCS}} = 1.2$ (0min after stimulation), $f_{\text{tDCS}} = 1.1$ (20min after stimulation) and $f_{\text{tDCS}} = 1.05$ (40min after stimulation). We have assumed a stimulation duration time of 12 min implying the plasticity time scale $\tau_{\text{plast}} = 1$ min and a decay of the plasticity effect with $\tau_{\text{decay}} = 30$ min. In addition, the excitatory synaptic efficacy to ARAS input is $f^{\text{resp}}_{\text{tDCS}} = f_{\text{tDCS}}$.

The model simulations also permit to predict population activity in the thalamic structures, cf. Fig. 5. We observe a relay cell population activity, which is very similar to the EEG activity. Conversely, the reticular population exhibits a much weaker $\gamma-$activity but a strong $\delta-$activity. The a-tDCS appears to have no impact on the activity of thalamic structures.

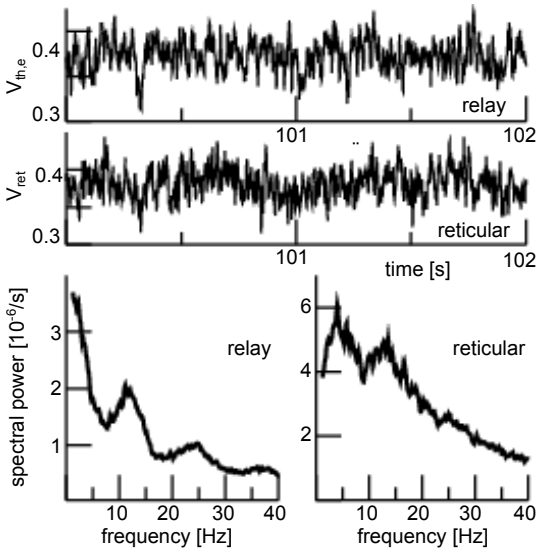

Figure 5. Long duration-anodal tDCS impact on subcortical activity. Upper panels: time series of simulated population activity for a-tDCS stimulation with $f_{\text{tDCS}} = 1.2$. Lower panels: spectral power density distribution of relay and reticular population activity in the absence (dashed line, $f_{\text{tDCS}} = 1.0$) and presence (solid line, $f_{\text{tDCS}} = 1.2$) of a-tDCS stimulation.

3.3. Impact of anodal tDCS in psychosis model

Previous experimental studies on humans [23,24] and rats [59,70,71] under ketamine have shown that the experimental setup represents a reasonable psychosis model. The subjects exhibit pathological ketamine-induced enhanced $\gamma-$ and diminished $\sigma-$ and

$\delta-$activity [20–24,60]. These spectral features resemble the power modulation in at risk mental state patients for psychosis. It has also been shown experimentally that an additional long duration-anodal tDCS stimulation reverses the impact of ketamine [60] which resembles the clinical impact of a-tDCS in human psychosis patients. Figure 6 presents EEG and subcortical activity in the control condition (no ketamine, no a-tDCS), under ketamine but no a-tDCS and in the presence of ketamine and a-tDCS. Under ketamine, the EEG power decrease in the $\delta-$ and $\sigma-$frequency range but increases in $\gamma-$ frequency range. The relay cell population responds similarly but the ketamine impact is less prominent. Conversely, in the reticular cell population ketamine enhances slightly spectral power in the $\delta-$frequency range only.
Now applying a-tDCS enhances EEG power in the $\delta-$ and $\sigma-$frequency band and moves the spectral EEG power from the $\gamma-$frequency band to lower frequencies. Relay cells respond to the a-tDCS by a similar power increase in the $\delta-$ and $\sigma-$frequency, while $\gamma-$activity is retained. In the reticular population, the a-tDCS stimulation enhances the $\delta-$power but does not affect the spectral power in larger frequencies.

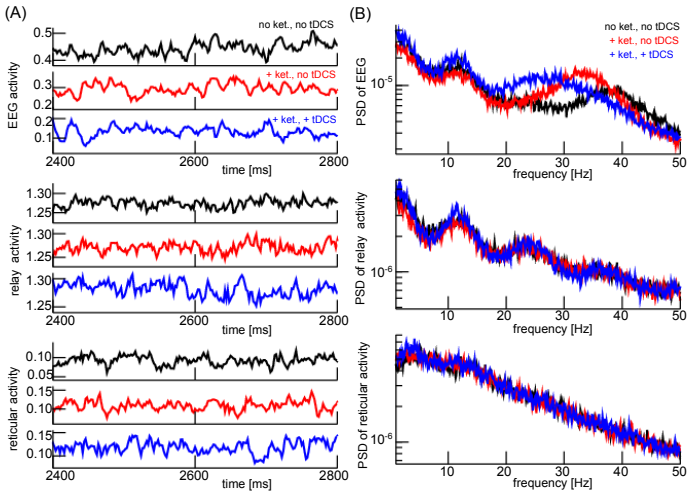

Figure 6. Cortical and subcortical activity under ketamine and anodal tDCS. (A) Model activity time courses of EEG (upper panels), relay cell population (center panels) and reticular cell population (lower panels) under different conditions. (B) Power spectral density distributions of EEG (top panel), relay cell population panel (center panel) and reticular cell population (bottom panel). Parameters are $f_{tDCS} = 1.05$ corresponding to stimulation duration of 4min with $\tau_{\text{plast}} = 1$ min, $f_{\text{ketamine}} = 0.7$ in the cortico-thalamic loop and $f_{\text{ketamine}} = 0.8$, $f_{tDCS}^{\text{resp}} = 2.0$ in SG layers.

These ketamine-induced effects are summarized in Fig. 7(A), where cortical and relay cell power decrease in the $\delta-$ and $\sigma-$ frequency band with ketamine, while ketamine enhances $\delta-$power in reticular cells. Additional a-tDCS stimulation enhances further cortical and relay cell population power in the $\delta-$ and $\sigma-$band, while the impact on reticular population is weak. Conversely, $\gamma-$activity is strongly enhanced by ketamine in cortical cells and diminished by a-tDCS. The sub-cortical $\gamma-$activity is poorly affected by the a-tDCS application. Despite a difference in the $\delta-$ band reticular response to ketamine, theses findings show good accordance to previous experimental findings in rodents [26,60] and patients suffering from schizophrenia [9].

To reveal more details on the brain dynamics in psychosis, functional connectivity between brain areas provide some insights [72,73]. We have computed the phase coherence in the CTC between their involved neural populations, cf. Fig. 7(B). Ketamine enhances FC in the $\delta-$frequency range between the cortical GIG, the relay and the reticular cells, while it diminishes FC in the $\sigma-$ range between these populations. The FC is also reduced between cortical and thalamic relay cells and between the thalamic structures in the $\gamma-$frequency

range under ketamine, whereas it does not affect the cortico-reticular connectivity. Now adding a-tDCS, FC increases between almost all areas and frequency bands, except in the intra-thalamic connections in the $\gamma-$band. Hence, a-tDCS inverses the ketamine FC reduction in the $\sigma-$band between all areas and in the $\gamma-$range between GIG layer cells and relay cells.

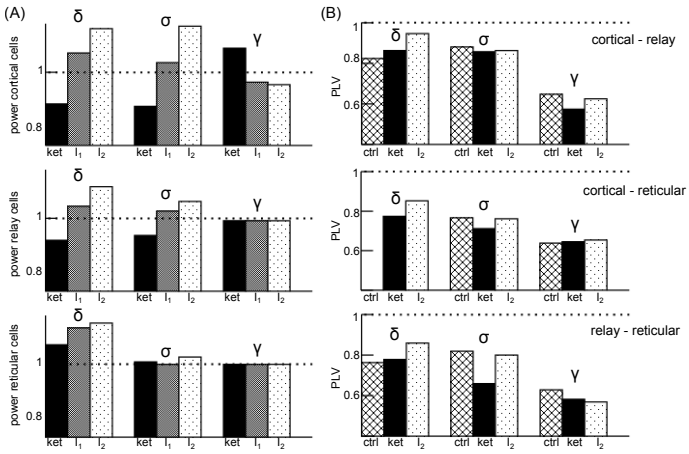

Figure 7. Relative spectral power and phase coherence PLV in the cortico-thalamic circuit. (A) The ratio of power spectral density averaged over frequencies in the corresponding frequency band and the corresponding average power spectral density in the control condition. The power in cortical cells consider GIG cells. (B) Degree of phase coherence (PLV) between excitatory cortical GIG population activity and the excitatory relay population activity (top panel), the excitatory cortical GIG layer and the reticular population activity (center panel) and between the reticular and relay cells (bottom panel). To notice, there is no cortico-reticular phase coherence in the basal condition. Model parameters are $f_{\text{tDCS}}^{\text{resp}} = 2.0$, $f_{\text{tDCS}} = 1.03$ and $f_{\text{tDCS}} = 1.05$ for stimulation input I_1 and $I_2 > I_1$, respectively. Ketamine parameters are identical to parameters used in Fig. 6.

4. Discussion

4.1. Excitability and spectral power

We present a neural population model which permits to reproduce major experimental EEG data features observed under tDCS. This model implies a cortico-thalamic feedback loop that generates the $\delta-$ and $\sigma-$rhythm. This loop includes GIG cortical cells, relay cells and reticular cells with corresponding excitatory and inhibitory synaptic connections. Moreover, a SG cell population is the origin of the $\gamma-$rhythm in good accordance with previous experimental results [74,75]. The reproduced features include an increased (decreased) excitability for a-tDCS (c-tDCS) in good agreement with previous experimental findings [47,49]. The presented excitability study is very brief and demonstrates a fundamental excitability modulation with tDCS. Future work should evaluate the presented evoked potential model much further, e.g. comparing modeling results to previous detailed expertimental results [76].

In addition, long duration a-tDCS enhances EEG power in good agreement with experimental studies in humans [9,67–69,77,78]. Our model assumes LTP-like long term potentiation of excitatory synapses and corresponding model simulations reproduce well the EEG power enhanced by a-tDCS. We propose to describe the rather complex neurophysiological plasticity effects by a simple modulation of the synaptic excitatory efficacy. Moreover, we present a stimulation-timing model that relates a temporal stimulation protocol with the plasticity effect. Future studies will evaluate this model by comparison to experimental tDCS effects as described in [79,80].

Since this model simplification reproduces EEG power features successfully, the present work supports the LTP-like effect of a-tDCS. The model also permits to predict the a-tDCS impact on thalamic cells and we find a poor effect on the thalamic power. Future experimental work will evaluate and verify this finding. As an additional well-known effect,

long-term impact of tDCS on the brain decays after some time. This effect is central in patients whose possibly successful tDCS impact decay after some months after treatment stop [5,8,9,44]. We have proposed a decay model of the plasticity effect which describes well the modulation of the tDCS after stimulation ends, cf. Figs. 3 and 4.
Several previous studies have modeled the electric field induced by tDCS [81–83]. Such studies provide some insights into the spatial location of tDCS impact, but does not allow to explain the dynamic impact on experimentally observed data. A different recent model study has focused on the tDCS impact on single neuron activity in neural populations considering homeostatic structural plasticity [84]. This impressive work takes into account different stimulation protocols in more detail than our work does. However it does not explain major tDCS effects on neural oscillatory brain activity that has been observed vastly in previous studies. The present work provides such an explanation in the context of psychosis taking into account recent neurophysiological hypothesis. Moreover, the ensemble model does not exhibit a realistic brain topology such as our CTC model and hence is less realistic concerning the brain network structure.

4.2. Spectral power in the psychosis model

We have further extended the neural model to describe EEG under psychosis assuming a ketamine model [25,27]. Identifying the brain state induced by ketamine with the psychotic state and the control brain state as a healthy state, we observe a drop of $\delta-$ and $\sigma-$power in the simulated EEG in the psychotic state compared to the healthy state. Conversely, the psychotic state exhibits a strong $\gamma-$ power enhancement. These findings are in good agreement with experimental data in humans [23–25] and rats [20–22]. Nevertheless, we also show an increase in the $\delta-$ power of reticular cells in the simulated psychotic state. This result defer from recent findings in which all CTC structures present a $\delta-$ power decrease after acute ketamine treatment [26,58]. Also, previous experimental studies have shown that a-tDCS may alleviate psychosis patients from symptoms [5,8,9,85]. Our model predicts an enhancement of $\delta-$ and $\sigma-$ power and a reduction of $\gamma-$ power by a-tDCS, which well replicate ancient experimental findings in an animal ketamine model [60].

4.3. Connectivity modulation in the psychosis model

The functional connectivity between brain areas reflects the brains ability to pass and share information between the structures. For instance, brain networks in mental disorders exhibit diminished FC between brain areas and thus a network fragmentation [86]. Enhanced functional dysconnectivity has been found in early psychosis [87] and reduced conscious access in psychosis is related to diminished long-range structural connectivity [88], then supporting the dysconnection hypothesis in schizophrenia [10,11]. This fragmentation can be reversed by psychotherapy in combination with a placebo or antipsychotics [89] and by a-tDCS [73]. It is interesting to note that a-tDCS not only enhances FC in psychosis patients but also in healthy subjects [90]. This indicates that a-tDCS may enhance brain FC in general. We have investigated this effect by computing FC in our neural model and found equivalent results. In the $\sigma-$ and $\gamma-$ frequency range, FC decreases in the ketamine model compared to the control condition. Conversely FC between all CTC structures increases in the $\delta-$ frequency band during the ketamine condition suggesting a $\delta-$ hypersynchronisation in the entire CTC network in the psychotic state. This new result adds to the previous finding of intra-thalamic $\gamma-$ synchronisation [26] driven by cortical "$\gamma-$ noise" [22]. Interestingly, for all frequency bands, a subsequent a-tDCS stimulation re-enhances FC. The only exception is the intra-thalamic FC in the $\gamma-$ range that decreases by a-tDCS.

4.4. Strength and limits of the neural model

The proposed model permits to reproduce experimental results on excitability and spectral power of EEG originating in cortical layers, as well as excitability and spectral

power of neural activity in non-cortical brain areas. Moreover, the model allows to predict FC in the cortico-thalamic circuit and elucidates how tDCS augments information sharing between brain areas. To gain these insights, the neural model considers recent hypothesis how tDCS affects synapses and neuronal populations. For instance, we assume that tDCS induces an intrinsic Poisson-noise activity in single neurons that represents a modulated input current and transfer function in the population [48]. This allows to describe the well-known modulated excitability by short duration-tDCS. Moreover, the simple assumption that long duration-anodal tDCS reflects an augmented excitatory synaptic efficacy in cortical neurons similar to the effect of LTP permits to describe the EEG power modulation under a-tDCS.

To describe the anodal tDCS-impact in psychosis-related prodrome, we present a neural ketamine model that considers both the hypofunction of NMDA receptors and the ketamine-induced disinhibition. Both mechanisms appear to be essential to reproduce the $\sigma-$power diminution and $\gamma-$enhancement found experimentally. Since ketamine both inhibits excitatory cells and inhibitory cells and the latter inhibition yields disinhibition of the population, it is an open question how the different power responses emerge. Our model explains this by actions in two sub-circuits. Neuronal populations in the cortico-thalamic loop, including granular/infragranular cortical layer, thalamic relay cells and reticular neurons, experience primarily the ketamine-induced hypofunction generating the power-diminished $\sigma-$rhythm. Simultaneously, the cortical supragranular layer neurons and the ARAS are affected by the ketamine-induced disinhibition. Since the thalamus and ARAS are known to project to the supragranular layer neurons generating the $\gamma-$rhythm [38], the ketamine-induced disinhibition yields a $\gamma-$power enhancement as observed experimentally.

Now recalling that a-tDCS has been found to enhance the brain, it appears counter-intuitive that the additional a-tDCS diminishes the $\gamma-$power in the ketamine model as shown experimentally [60]. To resolve this seeming contradiction, our simulations indicate that the combination of the cortical Poisson-neuron input and ARAS input in the supragranular layers yields a power shift from the $\gamma-$frequency range to lower frequencies, and hence a drop in $\gamma-$power. This power shift explains the $\gamma-$power drop, but remains to be shown experimentally.

The presented model is a rate-coding population model that considers firing rates of single neurons but neglects the timing of single spikes and spike train modes. This simplification is reasonable to describe mesoscopic population activity such as Local Field Potentials or EEG [33]. However, tDCS modulates both spike patterns and spike timing [91] and may affect the spectral power of neural populations without modulating neuron firing rates [92]. Our neural model does not describe such a spike train effect, making it unable to capture such rhythm modulations. This represents a limit of the population rate model.

Moreover, the model does not specify the underlying neuron type but implies a general type-I neuron [93]. It also does not specify details of intra- and inter-network connections, such as realistic spatial neural networks in single brain areas and topographic thalamo-cortical mapping. At a first glance, this may represent a strong limitation of the model and questions its validity. However, we argue that we are interested in the general underlying neural mechanism of tDCS and its impact in psychosis valid for all mammals. Since tDCS in different subjects of different mammalian species trigger similar EEG neural responses [44,51,65,66], it is important to choose a general rather simplistic population model that captures essential neural features and hence is independent of specific model choices. Here, the essential features are the nonlinear transfer function between synaptic input and population firing rate, realistic synaptic response models and a brain network topology of realistic polarity, i.e. with realistic excitation and inhibition. For instance, the emergence of a reticular $\delta-$activity observed in Fig. 4 matches experimental findings in the

thalamus [94,95] and results from the chosen network topology as shown previously [32].

Future work should improve the neural model by including neural mechanisms of spindles since these are known to represent important EEG markers in psychosis and their prodrome [26,96,97]. Incorporating spiking modes of the reticular population should allow to reproduce such dynamics, switching from bursting mode in the control/healthy condition to single action potential/tonic mode in the psychosis/ketamine condition [26]. In addition, there is strong evidence that the $\delta-$rhythm originates in the cortico-thalamic loop [98,99] and its role in psychosis remains to be revealed [100]. Future work will address the function and origin of $\delta-$rhythms in psychosis in more detail. Essentially, the present work demonstrates how to describe mathematically neurostimulation impact on EEG and how to predict brain activity. This may trigger models for other neurostimulation techniques over the scalp, such as transcranial Alternating Current Stimulation (tACS), transcranial Magnetic Stimulation (TMS) or cerebellar neurostimulation. Indeed, most neuromodulatory approaches have attracted increasing attention in recent years and seem to represent promising tools for future clinical treatment and prevention in psychiatry [101].

5. Conclusions

The present work provides a mathematical description of tDCS impact on brain activity in the context of psychosis and give track to improve experimental setups. To reproduce the ketamine-induced oscillopathies, usually used to mimic the schizophrenic prodrome-related EEG, the essential neural mechanisms are a reduced cortical inhibitory efficacy and an increased ARAS input to cortical structures. This supports the NMDA receptor hypofunction hypothesis in schizophrenia. Moreover, the simulation of tDCS influence on EEG can be achieved by simple modulation of synaptic efficacy, with a temporal dimension to mimic long-term plasticity effects. Finally, these findings support the idea that a-tDCS could reduce, or even normalize, schizophrenia prodrome-related oscillopathies, indicating its powerful potential as a preventive treatment.

Author Contributions: Conceptualization, J.R. and A.H.; methodology A.H.; software, A.H.; validation , J.R. and A.H.; formal analysis, A.H.; investigation, J.R. and A.H.; resources, J.R. and A.H.; data curation, J.R. and A.H.; writing—original draft preparation, J.R. and A.H.; writing—review and editing, J.R. and A.H.; visualization, A.H. All authors have read and agreed to the published version of the manuscript.

Funding: This research was funded by INRIA in the *Action Exploratoire* project *A/D Drugs*.

Acknowledgments: We acknowledge valuable discussions with Didier Pinault.

Conflicts of Interest: The authors declare no conflict of interest. The funders had no role in the design of the study, the collection, analyses, or interpretation of data, in the writing of the manuscript, or in the decision to publish the results.

Appendix A Mathemtical details of the population model

Appendix A.1 The population model

The model describes population activity in the cortex layers I-III and the cortico-thalamic loop between cortical layers IV-VI, the thalamic relay cells and the reticular structure. The layer I-III excitatory (inhibitory) mean potential is u (v), the excitatory (inhibitory) mean potential in the layer IV-VI neurons is denoted as V_e (V_i), the variables $V_{th,e}$ and $V_{th,i}$ denote excitatory and inhibitory mean potentials in the thalamic relay cells

and V_{ret} denotes the mean potential in the reticular structure. In a good approximation for large networks, these variables obey

$$\begin{aligned}
\tau_e \frac{dV_e(t)}{dt} &= -V_e(t) + F_e T_c[V_e(t) - V_i(t)] + F_{ct} T_{th}[V_{th,e}(t-\tau) - V_{th,i}(t-\tau)] \\
&\quad + F_{ccx} S_e[u(t)] + \mu_e + I_e + \rho_e(t) + c_1 I(t) \\
\tau_i \frac{dV_i(t)}{dt} &= -V_i(t) + F_i T_c[V_e(t) - V_i(t)] + \mu_i + I_i + \rho_i(t) + c_2 I(t) \\
\tau_{th,e} \frac{dV_{th,e}(t)}{dt} &= -V_{th,e}(t) + F_{tc} T_c[V_e(t) - V_i(t)] + \mu_{th,e} + \rho_{th,e}(t) \\
\tau_{th,i} \frac{dV_{th,i}(t)}{dt} &= -V_{th,i}(t) + F_{tr} T_{ret}[V_{ret}(t)] + \mu_{th,i} + \rho_{th,i}(t) \\
\tau_{ret} \frac{dV_{ret}(t)}{dt} &= -V_{ret}(t) + F_{rt} T_{th}[V_{th,e}(t) - V_{th,i}(t)] + F_{rc} T_c[V_e(t) - V_i(t)] + \mu_{ret} + \rho_{ret}(t) \\
\tau_{ce} \frac{du(t)}{dt} &= -u(t) + F^u_{cx} S_e[u(t)] - M^u_{cx} S_i[v(t)] \\
&\quad + F_{cx,th} T_{th}[V_{th,e}(t-\tau) - V_{th,i}(t-\tau)] + \mu_{ce} + I_{ce} + \rho_{ce}(t) + c_3 I(t) \\
\tau_{ci} \frac{dv(t)}{dt} &= -v(t) - F^v_{cx} S_i[v(t)] + M^v_{cx} S_e[u(t)] + \mu_{ci} + I_{ci} + \rho_{ci}(t) + c_4 I(t)
\end{aligned} \tag{A1}$$

with the transfer functions

$$T_m[x] = \frac{1}{2}\left(1 - \mathrm{erf}\left(-\frac{x}{\sqrt{2}\sigma_{\mathrm{m}}}\right)\right) \tag{A2}$$

$$S_m[x] = \frac{1}{2}\left(1 - \mathrm{erf}\left(-\frac{x}{\sqrt{2}\sigma_{\mathrm{cm}}}\right)\right) \tag{A3}$$

and the delay time τ in cortical-thalamic and cortical-reticular transmission. The noise $\rho_m(t)$ represents finite-size fluctuations and is uncorrelated in time, it is independent to other fluctuations $\xi_{n\neq m}(t)$, it has zero mean and variance D_x/N, i.e.

$$\langle \xi_x(t) \rangle = 0 \quad , \quad \langle \xi_x(t) \xi_y(t') \rangle = \frac{D_x}{N} \delta_{xy} \delta(t - t') \, .$$

Here, N is the number of neurons considered in the underlying network and D_x is the variance of the input noise in population $x = e,\ i,\ \{\mathrm{th,e}\},\ \{\mathrm{th,i}\},\ \mathrm{ret},\ ce,\ ci$.
We point out that the population model is a mean-field model originating from a neuron network [37,39,102–104] and additive noise input shapes the transfer functions T_m and S_m by the corresponding noise variance σ_{m}, σ_{cm}. In more detail, the variance σ^2_m in the transfer function (A2) is in a good approximation

$$\begin{aligned}
\sigma^2_c &= \frac{D_e}{\tau_e} + \frac{D_i}{\tau_i} \quad , \quad \sigma^2_{th} = \frac{D_{\mathrm{th,e}}}{\tau_{\mathrm{th,e}}} + \frac{D_{\mathrm{th,i}}}{\tau_{\mathrm{th,i}}} \quad , \quad \sigma^2_{ret} = \frac{D_{\mathrm{ret}}}{\tau_{\mathrm{ret}}} \\
\sigma^2_{ce} &= \frac{D_{ce}}{\tau_{ce}} \quad , \quad \sigma^2_{ci} = \frac{D_{ci}}{\tau_{ci}} \, .
\end{aligned}$$

Appendix A.2 Implementation of tDCS

To describe the impact of tDCS on the brain, it is important to distinguish short-term and long-term stimulation. For short stimulus periods, no plasticity effect occurs. Anodal tDCS induces an increased input current I and increased variances σ^2_c and σ^2_{ce} [39,48].
For long-term stimulation, we assume an increased excitatory synaptic efficacy in cortical layers with $F_e \to f_{\mathrm{tDCS}} F_e$, $F_{ct} \to f_{\mathrm{tDCS}} F_{ct}$, $F_{ccx} \to f_{\mathrm{tDCS}} F_{ccx}$, $\mu_e \to f_{\mathrm{tDCS}} \mu_e$, $I_e \to$

Table A1. Parameter set of model (A1).

parameter	description	value
τ_e	exc. decay time (infragranular)	10ms
τ_i	inh. decay time (infragranular)	50ms
$\tau_{th,e}$	exc. decay time (relay)	5ms
$\tau_{th,i}$	inh. decay time (relay)	30ms
τ_{ret}	exc. decay time (reticular)	8ms
τ_{ce}	exc. decay time (supragranular)	5ms
τ_{ci}	inh. decay time (supragranular)	20ms
τ	cortico-thalamic propagation delay	35ms
F_e	exc. synaptic strength	1.0
F_i	inh. synaptic strength	2.0
F_{ct}	synaptic strength (relay $\rightarrow$ cortex)	1.2
F_{tc}	synaptic strength (cortex $\rightarrow$ relay)	1.0
F_{tr}	synaptic strength (reticular $\rightarrow$ relay)	1.0
F_{rt}	synaptic strength (relay $\rightarrow$ reticular)	0.3
F_{rc}	synaptic strength (cortex $\rightarrow$ reticular)	0.6
F^u_{cx}	synaptic strength (exc. $\rightarrow$ exc.)	2.18
M^u_{cx}	synaptic strength (inh. $\rightarrow$ exc.)	3.88
F^v_{cx}	synaptic strength (inh. $\rightarrow$ inh.)	2.18
M^v_{cx}	synaptic strength (exc. $\rightarrow$ inh.)	3.88
F_{ccx}	synaptic strength (supragranular $\rightarrow$ infragranular)	0.05
$F_{cx,th}$	synaptic strength (thalamic relay $\rightarrow$ supragranular)	0.1
μ_e	exc. noise input (infragranular)	0.1
I_e	exc. resting input (infragranular)	0.2
μ_i	inh. noise input (infragranular)	0.0
I_i	inh. resting input (infragranular)	1.7
$\mu_{th,e}$	exc. noise input (relay)	1.2
$\mu_{th,i}$	inh. noise input (relay)	1.0
μ_{ret}	exc. noise input (reticular)	0.0
μ_{ce}	exc. noise input (supgragranular)	0.05
I_{ce}	exc. resting input (supragranular)	1.1
μ_{ci}	inh. noise input (supgragranular)	0.05
I_{ci}	inh. resting input (supragranular)	0.4
D_e	exc. input noise variance (infragranular)	$3 \cdot 10^{-5}$
D_i	inh. input noise variance (infragranular)	0.001
$D_{\mathrm{th,e}}$	exc. input noise variance (relay)	$2.5 \cdot 10^{-6}$
$D_{\mathrm{th,i}}$	inh. input noise variance (relay)	$12.6 \cdot 10^{-6}$
D_{ret}	exc. input noise variance (reticular)	$10.9 \cdot 10^{-6}$
D_{ce}	exc. input noise (supragranular)	$2 \cdot 10^{-5}$
D_{ci}	inh. input noise (supragranular)	$8 \cdot 10^{-5}$
N	number of neurons	1000

$f_{\mathrm{tDCS}} I_e$, $D_e \to f_{\mathrm{tDCS}} D_e$, $c_1 \to f_{\mathrm{tDCS}} c_1$ and $F^u_{cx} \to f_{\mathrm{tDCS}} F^u_{cx}$, $M^v_{cx} \to f_{\mathrm{tDCS}} M^v_{cx}$ and the plasticity factor $f_{\mathrm{tDCS}} > 1$.

The plasticity factor is chosen as a fixed value in the majority of simulations, but here we provide a model to describe how it may evolve in time during and after tDCS. Following the strong relation between synaptic plasticity and LTP which may originate from tDCS-induced neural synchronization, we assume that the plasticity effect reflects a certain degree of synchronization and thus is low for short tDCS and saturates at a maximum value for long tDCS. Then the growth of f_{tDCS} with stimulation time may obey the growth law of populations. With $f_{\mathrm{tDCS}} = 1 + f$ we postulate

$$\frac{df}{dt} = p(f) - d(f) \tag{A4}$$

with the plasticity birth process obeying a logistic equation

$$p(f) = \frac{I_0 f}{\tau_{\mathrm{plast}}} \left(1 - \frac{f}{f_{\mathrm{sat}} - 1}\right)$$

and the plasticity death or decay process

$$d(f) = -\frac{f}{\tau_{\mathrm{decay}}} .$$

The time constant τ_{plast} and τ_{decay} represent the time scale at which tDCS enhances and diminishes plasticity-induced excitation, respectively. Experiments show that plasticity is enhanced rather fast (tens of minutes) compared to long-term plasticity (hours and days). Hence, we choose $\tau_{\mathrm{plast}} \ll \tau_{\mathrm{decay}}$. Moreover, when tDCS is applied it is $I_0 = 1$ and otherwise $I_0 = 0$.

For illustration, neglecting the decay of plasticity ($\tau_{\mathrm{decay}} \to \infty$)

$$f_{\mathrm{tDCS}}(t) = 1 + \frac{f_{\mathrm{sat}} - 1}{1 + \frac{f_{\mathrm{sat}} - 1 - f_0}{f_0} e^{-t/\tau_{\mathrm{plast}}}}$$

where t is the stimulation time and f_0 is the initial plasticity $f_0 = f(t = 0)$. This is the logistic function shown in Fig. 3(A, left panel). For absent tDCS ($I_0 = 0$), the plasticity decays by

$$f_{\mathrm{tDCS}}(t) = f_0 e^{-t/\tau_{\mathrm{decay}}},$$

cf. Fig. 3(A, right panel).

In addition, model equation (A4) permits to describe the a-tDCS impact of a certain stimulation protocol with intermittent periods of stimulation. Fig. 3(B) shows solutions of model equation (A4) for different a-tDCS duration. According to typical a-tDCS stimulation protocols, one applies a-tDCS with a duration T_s (typically tens of minutes) and pauses between stimulations (typically several hours or days).

Appendix A.3 Implementation of evoked potentials

We assume an input current as a sum of a constant tDCS current $I_{tDCS} = \mathrm{const}$ and a time-dependent stimulus-evoked current $I_{EP}(t)$, i.e. $I(t) = I_{tTDCS} + I_{EP}(t)$. In addition, the evoked current affects the system transfer functions yielding $\sigma_c^2 \to \sigma_c^2 + \gamma_1 I(t)$ and $\sigma_{ce}^2 \to \sigma_{ce}^2 + \gamma_2 I(t)$, $\sigma_{ci}^2 \to \sigma_{ci}^2 + \gamma_3 I(t)$ with some factors γ_1, γ_2, $\gamma_3 > 0$.

The evoked stimulation $I_{EP}(t)$ is modeled as a sequence of periods with durations T with $I_E P = 0.05$, while these periods have an equally distributed random duration in the interval 180ms$\leq T \leq$ 220ms. The stimuli exhibit a random interstimulus interval ISI, which is equally distributed in the interval 370ms$\leq$ ISI $\leq$ 530ms. A simulation time of 90s yields $\sim$ 200 trials, whose average represents the Event-related Potential component (ERP). Its

magnitude illustrates the degree of excitability of the system, i.e. the larger is the response the more excitable the system is. Moreover, we define the baseline activity in the interval just 50ms before the stimulus onset in each trial. Its trial average indicates the system excitability as well, similar to the response magnitude, cf. Fig. 2.

Appendix A.4 Implementation of ketamine impact

The anesthetics ketamine is an antagonist of NMDA receptors [54,55] and affects the brain dopamine system [56]. Ketamine has several diverse actions. At sub-anesthetic doses in humans, it induces an hypofunction of NMDA receptors and increases the release of glutamate in cortical structures [105,106]. Similar results were found in rats [107]. This counterintuitive excitation effect could be due to the preferential and markedly inhibitory action of ketamine over GABAergic cortical interneurons [57] and thalamo-reticular neurons [26,58]. Since the NMDA hypofunction at GABAergic neurons diminishes their activity, an effective disinhibition of glutamatergic neurons of cortical layer IV and the thalamus is triggered. At subcortical levels, sub-anesthetic ketamine induces a discharge reduction in reticular and thalamic neurons [58]. According to previous experiments on rats [60], we assume sub-anesthetic doses implying a major disinhibition and an inhibition effect at NMDA receptors. In our model, we implement these effects by a factor $f_{ket} < 1$ in the cortical inhibitory efficacy parameter $F_i \to f_{ket} F_i$, in the excitatory cortico-thalamic connection to the relay cell population $F_{tc} \to f_{ket} F_{tc}$, in the inhibitory reticular-relay cell connection $F_{tr} \to f_{ket} F_{tr}$, in the excitatory relay-reticular connection $F_{rt} \to f_{ket} F_{rt}$ and the excitatory cortico-thalamic connection to the reticular structure $F_{rc} \to f_{ket} F_{rc}$. Moreover, ketamine diminishes the inhibitory synaptic efficacy in layers I-III and we choose $M^v_{cx} \to f_{ket} M^v_{cx}$.

In addition, the neurophysiological impact of ketamine proposes a strong disinhibition in subcortical structures, indicating an enhanced ARAS input to cortical structures [108,109]. Since cortical layers I-III receive ARAS input, we consider enhanced activity noise input to these layers. In our mathematical model, this input is taken into account by $\sigma_{ce} \sim 1/f_{\text{ket}}$, where σ_{ce} is the noise input variance to layer I-III neurons. Together with the excitatory plasticity factor for input response $f^{\text{resp}}_{\text{tDCS}} > 1$, we choose $\sigma_{ce} \to f^{\text{resp}}_{\text{tDCS}} / f_{\text{ket}} \sigma_{ce}$.

References

1. Durandeau, R. Évolution des états mentaux à risque de transition vers un trouble psychotique : une revue de la littérature. *DUMAS, Méd. humaine et pathologie* **2018**.
2. Collège National des Universitaires en Psychiatrie, A.p.l.d.l.S.P. *Référentiel ECN Psychiatrie et Addictologie*; Vol. Collection "l'Officiel ECN" 2ème édition, Presses Universitaires François Rabelais, France, 2016.
3. Millan, M.; Andrieux, A.; Bartzokis, G.; et al. Altering the course of schizophrenia: progress and perspectives. *Nat Rev Drug Discov* **2016**, *15*, 485–515.
4. Fusar-Poli, P.; Bonoldi, I.; Yung, A.; Borgwardt, S.; Kempton, M.; Valmaggia, L.; Barale, F.; Caverzasi, E.; McGuire, P. Predicting Psychosis: Meta-analysis of Transition Outcomes in Individuals at High Clinical Risk. *Arch Gen Psychiatry* **2012**, *69*, 220–229.
5. Chang, C.C.; Kao, Y.C.; Chao, C.Y.; Tzeng, N.S.; Chang, H.A. Examining bi-anodal transcranial direct current stimulation (tDCS) over bilateral dorsolateral prefrontal cortex coupled with bilateral extracephalic references as a treatment for negative symptoms in non-acute schizophrenia patients: A randomized, double-blind, sham-controlled trial. *Prog. in Neuro-Psychopharm. and Bio. Psych.* **2020**, *96*, 109715.
6. Coffman, B.A.; Clark, V.P.; Parasuraman, R. Battery powered thought: enhancement of attention, learning, and memory in healthy adults using transcranial direct current stimulation. *Neuroimage* **2014**, *85*, 895–908.
7. Mondino, M.; Jardri, R.; Suaud-Chagny, M.; Saoud, M.; Poulet, E.; Brunelin, J. Effects of Fronto-Temporal Transcranial Direct Current Stimulation on Auditory Verbal Hallucinations and Resting-State Functional Connectivity of the Left Temporo-Parietal Junction in Patients With Schizophrenia. *Schizophrenia Bull.* **2016**, *42*, 318–326.

8. Brunelin, J.; Mondino, M.; Gassab, L.; Haesebaert, F.; Gaha, L.; Suaud-Chagny, M.; Saoud, M.; Mechri, A.; Poulet, E. Examining transcranial direct-Current Stimulation (tdCS) as a treatment for Hallucinations in Schizophrenia. *Am. J. Psychiatry.* **2012**, *169*, 719–724.
9. Hoy, K.E.; Bailey, N.W.; Arnold, S.L.; Fitzgerald, P.B. The effect of transcranial direct current stimulation on gamma activity and working memory in schizophrenia. *Psych. Res.* **2015**, *228*, 191–196. doi:10.1016/j.psychres.2015.04.032.
10. Zhou, Y.; Fan, L.; Qiu, C.; Jiang, T. Prefrontal cortex and the dysconnectivity hypothesis of schizophrenia. *Neurosci. Bull.* **2015**, *31(2)*, 207–219.
11. Friston, K.; Brown, H.R.; Siemerkus, J.; Stephan, K.E. The dysconnection hypothesis (2016). *Schizophr. Res.* **2016**, *176*, 83–94.
12. Ramyead, A.; Kometer, M.; Studerus, E.; Koranyi, S.; Ittig, S.; Gschwandtner, U.; Fuhr, P.; Riecher-Rössler, A. Aberrant Current Source-Density and Lagged Phase Synchronization of Neural Oscillations as Markers for Emerging Psychosis. *Schizophrenia Bull.* **2015**, *41*, 919–929.
13. Reilly, T.J.; Nottage, J.F.; Studerus, E.; Rutigliano, G.; Micheli, A.I.D.; Fusar-Poli, P.; McGuire, P. Gamma band oscillations in the early phase of psychosis: A systematic review. *Neurosci. Behav. Rev.* **2018**, *90*, 381–399.
14. Fryer, S.L.; Roach, B.J.; Wiley, K.; Loewy, R.L.; Ford, J.M.; Mathalon, D.H. Reduced Amplitude of Low-Frequency Brain Oscillations in the Psychosis Risk Syndrome and Early Illness Schizophrenia. *Neuropsychopharmacol.* **2016**, *41*, 2388–2398.
15. Castelnovo, A.; Graziano, B.; Ferrarelli, F.; D'Agostino, A. Sleep spindles and slow waves in schizophrenia and related disorders: main findings, challenges and future perspectives. *Eur. J. Neurosci.* **2018**, *48*, 2738–2758.
16. Manoach, D.S.; Demanuele, C.; Wamsley, E.J.; Vangel, M.; Montrose, D.M.; Miewald, J.; Kupfer, D.; Buysse, D.; Stickgold, R.; Keshavan, M.S. Sleep spindle deficits in antipsychotic-naïve early course schizophrenia and in non-psychotic first-degree relatives. *Front. Hum. Neurosci.* **2014**, *8*, 762.
17. Tesler, N.; Gerstenberg, M.; Franscini, M.; Jenni, O.G.; Walitza, S.; Huber, R. Reduced sleep spindle density in early onset schizophrenia: A preliminary finding. *Schizophr. Res.* **2015**, *166*, 355–357.
18. Krystal, J.H.; Karper, L.; Seibyl, J.; Freeman, G.; Delaney, R.; Bremmer, D.; Heninger, G.; Bowers, M.; Charney, D. Subanesthetic Effects of the Noncompetitive NMDA Antagonist, Ketamine, in Humans. *Arch. Gen. Psychiatry* **1994**, *51*, 199–214.
19. Lahti, A.C.; Weiler, M.A.; Michaelidis, T.; Parwani, A.; Tamminga, C.A. Effects of Ketamine in Normal and Schizophrenic Volunteers. *Neuropsychopharmacol.* **2001**, *25*, 455–467.
20. Pinault, D. N-methyl d-aspartate receptor antagonists ketamine and MK-801 induce wake-related aberrant gamma oscillations in the rat neocortex. *Biol. Psychiatry* **2008**, *63*, 730–735.
21. Hakami, T.; Jones, N.C.; Tolmacheva, E.A.; Gaudias, J.; Chaumont, J.; Salzberg, M.; O'Brien, T.J.; Pinault, D. NMDA receptor hypofunction leads to generalized and persistent aberrant γ oscillations independent of hyperlocomotion and the state of consciousness. *PLOS ONE* **2009**, *4*, e6755.
22. Anderson, P.M.; Jones, N.C.; O'Brien, T.J.; Pinault, D. The N-Methyl D-Aspartate Glutamate Receptor Antagonist Ketamine Disrupts the Functional State of the Corticothalamic Pathway. *Cerebral Cortex* **2017**, *27*, 3172–3185.
23. Hong, L.; Summerfelt, A.; Buchanan, R.; O'Donnell, P.; Thaker, G.; Weiler, M.; Lahti, A. Gamma and delta neural oscillations and association with clinical symptoms under subanesthetic ketamine. *Neuropsychopharmacol.* **2010**, *35*, 632–640.
24. De la Salle, S.; Choueiry, J.; Shah, D.; Bowers, H.; McIntosh, J.; Ilivitsky, V.; Knott, V. Effects of Ketamine on Resting-State EEG Activity and Their Relationship to Perceptual/Dissociative Symptoms in Healthy Humans. *Front. Pharmacol.* **2016**, *7*, 348. doi:10.3389/fphar.2016.00348.
25. Haaf, M.; Leicht, G.; Curic, S.; Mulert, C. Glutamatergic Deficits in Schizophrenia - Biomarkers and Pharmacological Interventions within the Ketamine Model. *Curr. Pharm. Biotechnol.* **2018**, *19*, 293–307. doi:10.2174/1389201019666180620112528.
26. Mahdavi, A.; Qin, Y.; Aubry, A.S.; Cornec, D.; Kulikova, S.; Pinault, D. A single psychotomimetic dose of ketamine decreases thalamocortical spindles and delta oscillations in the sedated rat. *Schizophr. Res.* **2020**, *222*, 362–374.
27. Frohlich, J.; Van Horn, J.D. Reviewing the ketamine model for schizophrenia. *Psychopharm.* **2014**, *28*, 287–302.
28. Uno, Y.; Coyle, J.T. Glutamate hypothesis in schizophrenia. Psychiatry. *Clin. Neurosci.* **2019**, *73*, 204–215.

29. Niedermayer, E.; Lopes da Silva, F., Eds. *Electroencephalography: Basic Principles, Clinical Applications, and Related Fields*; Lippincott, Williams and Williams, 2005.
30. Nunez, P.; Srinivasan, R. *Electric Fields of the Brain: The Neurophysics of EEG*; Oxford University Press, New York - Oxford, 2006.
31. Robinson, P.; C.J.Rennie.; D.L.Rowe.; S.C.O'Connor. Estimation of Multiscale Neurophysiologic Parameters by Electroencephalographic means. *Human Brain Mapping* **2004**, *23*, 53–72.
32. Hashemi, M.; Hutt, A.; Sleigh, J. How the cortico-thalamic feedback affects the EEG power spectrum over frontal and occipital regions during propofol-induced anaesthetic sedation. *J. Comput. Neurosci.* **2015**, *39*, 155.
33. Deco, G.; Jirsa, V.; Robinson, P.; Breakspear, M.; Friston, K. The dynamic brain: from spiking neurons to neural masses and cortical fields. *PLoS Computational Biology* **2008**, *4*, e1000092.
34. Edlow, B.; Takahashi, E.; Wu, O.; Benner, T.; Dai, G.; Bu, L.; Grant, P.; Greer, D.; Greenberg, S.; Kinney, H.; et al. Neuroanatomic Connectivity of the Human Ascending Arousal System Critical to Consciousness and Its Disorders. *J. Neuropathol. Exp. Neurol.* **2012**, *71*, 531–546. doi:10.1097/NEN.0b013e3182588293.
35. Fuller, P.; Sherman, D.; Pedersen, N.; Saper, C.; Lu, J. Reassessment of the structural basis of the ascending arousal system. *J. Comput. Neurol.* **2011**, *519*, 933–956. doi:10.1002/cne.22559.
36. Robinson, P.; Loxley, P.; O'Connor, S.; Rennie, C. Modal analysis of corticothalamic dynamics, electroencephalographic spectra and evoked potentials. *Phys. Rev. E* **2001**, *63*, 041909.
37. Hutt, A.; Lefebvre, J.; Hight, D.; Sleigh, J. Suppression of underlying neuronal fluctuations mediates EEG slowing during general anaesthesia. *Neuroimage* **2018**, *179*, 414–428.
38. Hutt, A.; Lefebvre, J. Arousal fluctuations govern oscillatory transitions between dominant γ and α occipital activity during eyes open/closed conditions. *Brain Topography* **2021**, *in press*. doi:10.1007/s10548-021-00855-z.
39. Hutt, A.; Wahl, T.; Voges, N.; Hausmann, J.; Lefebvre, J. Coherence resonance in random Erdos-Renyi neural networks : mean-field theory. *Front. Appl. Math, Stat.* **2021**, *7*, 697904. doi:10.3389/fams.2021.697904.
40. Buffalo, E.; Fries, P.; Landman, R.; Buschman, T.; Desimone, R. Laminar differences in gamma and alpha coherence in the ventral stream. *Proc. Natl. Acad. Sci.* **2011**, *108*, 11262–11267.
41. Halgren, M.; Ulbert, I.; Bastuji, H.; Fabó, D.; Erőss, L.; Rey, M.; Devinsky, O.; Doyle, W.; Mak-McCully, R.; Halgren, E.; et al. The generation and propagation of the human alpha rhythm. *Proc. Natl. Acad. Sci. USA* **2019**, *116*, 23772–23782. doi:10.1073/pnas.1913092116.
42. Bartos, M.; Vida, I.; Jonas, P. Synaptic mechanisms of synchronized gamma oscillations in inhibitory interneuron networks. *Nature Rev. Neurosci.* **2007**, *8*, 45–56.
43. Stagg, C.; Antal, A.; Nitsche, M. Physiology of Transcranial Direct Current Stimulation. *J. ECT* **2018**, *34*, 144–152.
44. Brunoni, A.; Nitsche, M.; Bolognini, N.; Bikson, M.; Wagner, T.; Merabet, L.; Edwards, D.J.; Valero-Cabre, A.; Rotenberg, A.; Pascual-Leone, A.; et al. Clinical research with transcranial direct current stimulation (tDCS): Challenges and future directions. *Brain Stimulation* **2012**, *5*, 175–195.
45. Ferrucci, R.; Bortolomasi, M.; Vergari, M.; Tadini, L.; Salvoro, B.; Giacopuzzi, M.; Barbieri, S.; Priori, A. Transcranial direct current stimulation in severe, drug-resistant major depression. *J. Affect. Disorders* **2009**, *118*, 215–219. doi:10.1016/j.jad.2009.02.015.
46. Kayarian, F.B.; Jannati, A.; Rotenberg, A.; Santarnecchi, E. Targeting Gamma-Related Pathophysiology in Autism Spectrum Disorder using Transcranial Electrical Stimulation: Opportunities and Challenges. *Autism Res.* **2020**, *13*, 1051–1071. doi:10.1002/aur.2312.
47. Nitsche, M.A.; Paulus, W. Excitability changes induced in the human motor cortex by weak transcranial direct current stimulation. *J. Physiol.* **2000**, *527*, 633–639.
48. Hutt, A.; Wahl, T. Poisson-distributed noise induces cortical γ-activity: explanation of γ-enhancement by anaesthetics ketamine and propofol. *J. Phys. : Complexity* **2021**, *accepted*.
49. Romero Lauro, L.J.; Rosanova, M.; Mattavelli, G.; Convento, S.; Pisoni, A.; Opitz, A.; Bolognini, N.; Vallar, G. TDCS increases cortical excitability: Direct evidence from TMS–EEG. *Cortex* **2014**, *58*, 99–111. doi:https://doi.org/10.1016/j.cortex.2014.05.003.
50. Nitsche, M.A.; Paulus, W. Sustained excitability elevations induced by transcranial DC motor cortex stimulation in humans. *Neurology* **2001**, *57*, 1899–1901.
51. Jackson, M.P.; Rahman, A.; Lafon, B.; Kronberg, G.; Ling, D.; Parra, L.C.; Bikson, M. Animal Models of transcranial Direct Current Stimulation: Methods and Mechanisms. *Clin. Neurophysiol.* **2016**, *127*, 3425–3454. doi:10.1016/j.clinph.2016.08.016.

52. Korai, S.A.; Ranieri, F.; Di Lazzaro, V.; Papa, M.; Cirillo, G. Neurobiological After-Effects of Low Intensity Transcranial Electric Stimulation of the Human Nervous System: From Basic Mechanisms to Metaplasticity. *Front. Neurol.* **2021**, *12*, 587771. doi:10.3389/fneur.2021.587771.
53. Frase, L.; Mertens, L.; Krahl, A.; Bhatia, K.; Feige, B.; Heinrich, S.P.; Vestring, S.; Nissen, C.; Domschke, K.; Bach, M.; et al. Transcranial direct current stimulation induces long-term potentiation-like plasticity in the human visual cortex. *Transl. Psych.* **2021**, *11*, 17. doi:10.1038/s41398-020-01134-4.
54. Alkire, M.; Hudetz, A.; G.Tononi. Consciousness and Anesthesia. *Science* **2008**, *322*, 876–880. doi:10.1126/science.1149213.
55. McMillan, R.; Muthukumaraswamy, S.D. The neurophysiology of ketamine: an integrative review. *Rev. Neurosci.* **2020**, *31*, 457–503.
56. Matthysse, S. Antipsychotic drug actions: a clue to the neuropharmacology of schizophrenia? *Fed. Proc.* **1973**, *32*, 200–205.
57. Homayoun, H.; Moghaddam, B. NMDA receptor hypofunction produces opposite effects on prefrontal cortex interneurons and pyramidal neurons. *J. NBeurosci.* **2007**, *27*, 11496–11500.
58. Amat-Foraster, M.; Jensen, A.; Plath, N.; Herrik, K.; Celada, P.; Artigas, F. Temporally dissociable effects of ketamine on neuronal discharge and gamma oscillations in rat thalamo-cortical networks. *Neuropharmacology* **2018**, *137*, 13–23.
59. Mahdavi, A.; Qin, Y.; Aubry, A.S.; Cornec, D.; Kulikova, S.; Pinault, D. Sleep-related thalamocortical spindles and delta oscillations are reduced during a ketamine-induced psychosis-relevant transition state. *preprint* **2019**. doi:10.1101/833459.
60. Lahogue, C.; Pinault, D. Frontoparietal anodal tDCS reduces ketamine-induced oscillopathies. *Transl. Neurosci.* **2021**, *12*, 282–296. doi:10.1515/tnsci-2020-0157.
61. Bastos, A.; Schoffelen, J.M. A Tutorial Review of Functional Connectivity Analysis Methods and Their Interpretational Pitfalls. *Front. Syst. Neurosci.* **2016**, *9*, 175. doi:10.3389/fnsys.2015.00175.
62. Hutt, A.; Munk, M. Mutual phase synchronization in single trial data. *Chaos and Complexity Letters* **2006**, *2*, 6.
63. Lachaux, J.P.; Rodriguez, E.; Martinerie, J.; Varela, F. Measuring phase synchrony in brain signals. *Human Brain Mapp.* **1999**, *8*, 194–208.
64. Powanwe, A.; Longtin, A. Mechanisms of Flexible Information Sharing through Noisy Oscillations. *Biology* **2021**, *10*, 764. doi:10.3390/biology10080764.
65. Yamada, Y.; Sumiyoshi, T. Preclinical Evidence for the Mechanisms of Transcranial Direct Current Stimulation in the Treatment of Psychiatric Disorders; A Systematic Review. *Clin EEG Neurosci* **2021**, *in press*. doi:10.1177/15500594211066151.
66. Nitsche, M.A.; Cohen, L.G.; Wassermann, E.M.; Priori, A.; Lang, N.; Antal, A.; Paulus, W.; Hummel, F.; Boggio, P.S.; Fregni, F.; et al. Transcranial direct current stimulation: State of the art 2008. *Brain Stimulation* **2008**, *1*, 206–223.
67. Marshall, L.; Helgadóttir, H.; Mölle, M.; Born, J. Boosting slow oscillations during sleep potentiates memory. *Nature* **2006**, *444*, 610–613.
68. Paßmann, S.; Külzow, N.; Ladenbauer, J.; Antonenko, D.; Grittner, U.; Tamm, S.; Flöel, A. Boosting Slow Oscillatory Activity Using tDCS during Early Nocturnal Slow Wave Sleep Does Not Improve Memory Consolidation in Healthy Older Adults. *Brain Stimulation* **2016**, *9*, 730–739.
69. Donaldson, P.H.; Kirkovski, M.; Yang, J.S.; Bekkali, S.; Enticott, P.G. High-definition tDCS to the right temporoparietal junction modulates slow-wave resting state power and coherence in healthy adults. *J. Neurophysiol.* **2019**, *112*, 1735–1744.
70. Chatterjee, M.; Verma, R.; Ganguly, S.; Palit, G. Neurochemical and molecular characterization of ketamine-induced experimental psychosis model in mice. *Neuropharmacology* **2012**, *63*, 1161–1171.
71. Becker, A.; Peters, B.; Schroeder, H.; Mann, T.; Huether, G.; Grecksch, G. Ketamine-induced changes in rat behaviour: A possible animal model of schizophrenia. *Prog. Neuropsychopharmacol. Biol. Psychiatry* **2003**, *27*, 687–700. doi:10.1016/S0278-5846(03)00080-0.
72. Polania, R.; Nitsche, M.; Paulus, W. Modulating functional connectivity patterns and topological functional organization of the human brain with transcranial direct current stimulation. *Hum. Brain Map.* **2011**, *32*, 1236–1249. doi:10.1002/hbm.21104.
73. Yoon, Y.B.; Kim, M.; Lee, J.; Cho, K.; Kwak, S.; Lee, T.; Kwon, J.S. Effect of tDCS on Aberrant Functional Network Connectivity in Refractory Hallucinatory Schizophrenia: A Pilot Study. *Psychiatry Investig* **2019**, *16*, 244–248. doi:10.30773/pi.2018.11.18.

74. Bastos, A.; Briggs, F.; Alitto, H.; Mangun, G.; Usrey, W. Simultaneous Recordings from the Primary Visual Cortex and Lateral Geniculate Nucleus Reveal Rhythmic Interactions and a Cortical Source for Gamma-Band Oscillations. *J. Neurosci.* **2014**, *34*, 7639–7644. doi:10.1523/JNEUROSCI.4216-13.2014.
75. Whittington, M.A.; Cunningham, M.O.; LeBeau, F.E.; Racca, C.; Traub, R.D. Multiple Origins of the Cortical Gamma Rhythm. *Developmental Neurobiology* **2011**, *71*, 92–106.
76. Ahn, S.; Fröhlich, F. Pinging the brain with transcranial magnetic stimulation reveals cortical reactivity in time and space. *Brain Stimulation* **2021**, *14*, 304–315. doi:https://doi.org/10.1016/j.brs.2021.01.0
77. Venkatakrishnan, A.; Contreras-Vidal, J.; Sandrini, M.; Cohen, L.G. Independent component analysis of resting brain activity reveals transient modulation of local cortical processing by transcranial direct current stimulation. *Conf Proc IEEE Eng Med Biol Soc* **2011**, *2011*, 8102–8105.
78. Wilson, T.W.; McDermott, T.J.; Mills, M.S.; Coolidge, N.M.; Heinrichs-Graham, E. tDCS Modulates Visual Gamma Oscillations and Basal Alpha Activity in Occipital Cortices: Evidence from MEG. *Cerebral Cortex* **2018**, *28*, 1597–1609.
79. Monte-Silva, K.; Kuo, M.F.; Hessenthaler, S.; Fresnoza, S.; Liebetanz, D.; Paulus, W.; Nitsche, M. Induction of Late LTP-Like Plasticity in the Human Motor Cortex by Repeated Non-Invasive Brain Stimulation. *Brain Stimulation* **2013**, *6*, 424–432. doi:https://doi.org/10.1016/j.brs.2012.04.011
80. Agboada, D.; Mosayebi-Samani, M.; Kuo, M.F.; Nitsche, M. Induction of long-term potentiation-like plasticity in the primary motor cortex with repeated anodal transcranial direct current stimulation – Better effects with intensified protocols? *Brain Stimulation* **2020**, *13*, 987–997. doi:https://doi.org/10.1016/j.brs.2020.04.009.
81. Ciechanski, P.; Carlson, H.; Yu, S.; Kirton, A. Modeling Transcranial Direct-Current Stimulation-Induced Electric Fields in Children and Adults. *Front. Hum. Neurosci.* **2018**, *12*, 268. doi:10.3389/fnhum.2018.00268.
82. Bikson, M.; Rahman, A.; Datta, A. Computational models of transcranial direct current stimulation. *Clin. EEG Neurosci.* **2012**, *43*, 176–183. doi:10.1177/1550059412445138.
83. Ruffini, G.; Wendling, F.; Merlet, I.; Molaee-Ardekani, B.; Mekonnen, A.; Salvador, R.; Soria-Frisch, A.; Grau, C.; Dunne, S.; Miranda, P. Transcranial current brain stimulation (tCS): models and technologies. *IEEE Trans Neural Syst Rehabil Eng.* **2013**, *21*, 333–345. doi:10.1109/TNSRE.2012.2200046.
84. Lu, H.; Gallinaro, J.; Rotter, S. Network remodeling induced by transcranial brain stimulation: A computational model of tDCS-triggered cell assembly formation. *Network Neurosci.* **2019**, *3*, 924–943. doi:10.1162/netn_a_00097.
85. Yokoi, Y.; Narita, Z.; Sumiyoshi, T. Transcranial Direct Current Stimulation in Depression and Psychosis: A Systematic Review. *Clin EEG Neurosci* **2018**, *49*, 93–102. doi:10.1177/1550059417732247.
86. Hutt, A. Brain Connectivity Reduction Reflects Disturbed Self-Organisation of the Brain: Neural Disorders and General Anaesthesia. In *Multiscale models of Brain Disorders*; Cutsuridis, V., Ed.; Springer-Verlag, Berlin, 2019; pp. 207–218.
87. Griffa, A.; Baumann, P.; Klauser, P.; Mullier, E.; Cleusix, M.; Jenni, R.; van den Heuvel, M.; Do, K.; Conus, P.; Hagmann, .P. Brain connectivity alterations in early psychosis: from clinical to neuroimaging staging. *Transl Psychiatry* **2019**, *9*, 62. doi:10.1038/s41398-019-0392-y.
88. Berkovitch, L.; Charles, L.; Del Cul, A.; Hamdani, N.; Delavest, M.; Sarrazin, S.; Mangin, J.F.; Guevara, P.; Ji, E.; d'Albis, M.A.; et al. Disruption of Conscious Access in Psychosis Is Associated with Altered Structural Brain Connectivity. *J. Neurosci.* **2021**, *41*, 513–523. doi:10.1523/JNEUROSCI.0945-20.2020.
89. Chopra, S.; Francey, S.; O'Donoghue, B.; Sabaroedin, K.; Arnatkeviciute, A.; Cropley, V.; Nelson, B.; Graham, J.; Baldwin, L.; Tahtalian, S.; et al. Functional Connectivity in Antipsychotic-Treated and Antipsychotic-Naive Patients With First-Episode Psychosis and Low Risk of Self-harm or Aggression: A Secondary Analysis of a Randomized Clinical Trial. *JAMA Psychiatry* **2021**, *78*, 994–1004. doi:10.1001/jamapsychiatry.2021.1422.
90. Abellaneda-Perez, K.; Vaque-Alcazar, L.; Perellon-Alfonso, R.; Bargallo, N.; Kuo, M.F.; Pascual-Leone, A.; Nitsche, M.; Bartres-Faz, D. Differential tDCS and tACS Effects on Working Memory-Related Neural Activity and Resting-State Connectivity. *Front. Neurosci.* **2020**, *13*, 1440. doi:10.3389/fnins.2019.01440.
91. Reato, D.; Rahman, A.; Bikson, M.; Parra, L. Low-intensity electrical stimulation affects network dynamics by modulating population rate and spike timing. *J. Neurosci.* **2010**, *30*, 15067–15079. doi:10.1523/JNEUROSCI.2059-10.2010.

92. Krause, M.; Zanos, T.; Csorba, B.; Pilly, P.; Choe, J.; Phillips, M.; Datta, A.; Pack, C. Transcranial Direct Current Stimulation Facilitates Associative Learning and Alters Functional Connectivity in the Primate Brain. *Curr. Biol.* **2017**, *27*, 3086–3096. doi:10.1016/j.cub.2017.09.020.
93. Hutt, A.; Buhry, L. Study of GABAergic extra-synaptic tonic inhibition in single neurons and neural populations by traversing neural scales: application to propofol-induced anaesthesia. *J. Comput. Neurosci.* **2014**, *37*, 417–437.
94. Pinault, D. The thalamic reticular nucleus: structure, function and concept. *Brain Res. Rev.* **2004**, *46*, 1–31.
95. Destexhe, A.; Contreras, D. The Fine Structure of Slow-Wave Sleep Oscillations: from Single Neurons to Large Networks. In *Sleep and Anesthesia: Neural Correlates in Theory and Experiment*; Hutt, A., Ed.; Springer-Verlag, New York, 2011; pp. 69–105.
96. Au, C.; Harvey, C.J. Systematic review: the relationship between sleep spindle activity with cognitive functions, positive and negative symptoms in psychosis. *Sleep Medicine: X* **2020**, *2*, 100025. doi:10.1016/j.sleepx.2020.100025.
97. Ferrarelli, F.; Huber, R.; Peterson, M.J.; Massimini, M.; Murphy, M.; Riedner, B.A.; Watson, A.; Bria, P.; Tononi, G. Reduced sleep spindle activity in schizophrenia patients. *Am. J. Psychiatry* **2007**, *164*, 483–492.
98. Pinault, D. A Neurophysiological Perspective on a Preventive Treatment against Schizophrenia Using Transcranial Electric Stimulation of the Corticothalamic Pathway. *Brain Sci.* **2017**, *7*, 34. doi:10.3390/brainsci7040034.
99. Steriade, M.; Dossi, R.; Pare, D.; Oakson, G. Fast oscillations (20-40 Hz) in thalamocortical systems and their potentiation by mesopontine cholinergic nuclei in the cat. *Proc. Natl. Acad. Sci. USA* **1991**, *88*, 4396–4400.
100. Steullet, P. Thalamus-related anomalies as candidate mechanism-based biomarkers for psychosis. *Schizophrenia Research* **2020**, *226*, 147–157. doi:10.1016/j.schres.2019.05.027.
101. Escelsior, A.; Belvederi Murri, M.; Calcagno, P.; Cervetti, A.; Caruso, R.; Croce, E.; Grassi, L.; Amore, M. Effectiveness of Cerebellar Circuitry Modulation in Schizophrenia. *J. Nerv. Ment. Disease* **2019**, *207*, 977–986. doi:10.1097/NMD.0000000000001064.
102. Hutt, A.; Mierau, A.; Lefebvre, J. Dynamic Control of Synchronous Activity in Networks of Spiking Neurons. *PLoS One* **2016**, *11*, e0161488. doi:10.1371/journal.pone.0161488.
103. Hutt, A.; Lefebvre, J. Additive Noise Tunes the Self-Organization in Complex Systems. In *Synergetics*; Hutt, A.; Haken, H., Eds.; Encyclopedia of Complexity and Systems Science Series, Springer, New York, 2020.
104. Lefebvre, J.; Hutt, A.; Knebel, J.; Whittingstall, K.; Murray, M. Stimulus statistics shape oscillations in nonlinear recurrent neural networks. *J. Neurosci.* **2015**, *35*, 2895–2903.
105. Abdallah, C.; De Feyter, H.; Averill, L.; Jiang, L.; Averill, C.; Chowdhury, G.; Purohit, P.; de Graaf, R.; Esterlis, I.; Juchem, C. The effects of ketamine on prefrontal glutamate neurotransmission in healthy and depressed subjects. *Neuropsychopharm.* **2018**, *43*, 2154–2160. doi:10.1038/s41386-018-0136-3.
106. Rowland, L.; Bustillo, J.; Mullins, P.; Jung, R.; Lenroot, R.; Landgraf, E.; Yeo, R.B.R.; Lauriello, J.; Brooks, W. Effects of ketamine on anterior cingulate glutamate metabolism in healthy humans: a 4-T proton MRS study. *Am. J. Psychiatry* **2005**, *162*, 394–396.
107. Moghaddam, B.; Adams, B.; Verma, A.; Daly, D. Activation of glutamatergic neurotransmission by ketamine: a novel step in the pathway from NMDA receptor blockade to dopaminergic and cognitive disruptions associated with the prefrontal cortex. *J. Neurosci.* **1997**, *17*, 2921–2927.
108. Dawson, N.; Morris, B.J.; Pratt, J.A. Subanaesthetic ketamine treatment alters prefrontal cortex connectivity with thalamus and ascending subcortical systems. *Schizophr. Bull.* **2013**, *39*, 366–377.
109. Munk, M.; Roelfsema, P.; Konig, P.; Engel, A.; Singer, W. Role of reticular activation in the modulation of intracortical synchronization. *Science* **1996**, *272*, 271–274.